

# Evidence for Merger-Driven Activity in the Clustering of High Redshift Quasars

J. Stuart B. Wyithe<sup>1</sup> and Abraham Loeb<sup>2</sup>

<sup>1</sup> *School of Physics, University of Melbourne, Parkville, Victoria, Australia*

<sup>2</sup> *Harvard-Smithsonian Center for Astrophysics, 60 Garden St., Cambridge, MA 02138*

*Email: swyithe@unimelb.edu.au, loeb@cfa.harvard.edu*

30 October 2018

## ABSTRACT

Recently, a very large clustering length has been measured for quasars at a redshift of  $z \sim 4$ . In combination with the observed quasar luminosity function we assess the implications of this clustering for the relationship between quasar luminosity and dark matter halo mass. Our analysis allows for non-linearity and finite scatter in the relation between quasar luminosity and halo mass, as well as a luminosity dependent quasar lifetime. The additional novel ingredient in our modelling is the allowance for an excess in the observed bias over the underlying halo bias owing to the merger driven nature of quasar activity. We find that the observations of clustering and luminosity function can be explained only if both of the following conditions hold: *(i)* The luminosity to halo mass ratio increases with halo mass; *(ii)* The observed clustering amplitude is in excess of that expected solely from halo bias. The latter result is statistically significant at the 99% level. Taken together, the observations provide compelling evidence for merger driven quasar activity, with a black-hole growth that is limited by feedback. In difference from previous analyses, we show that there could be scatter in the luminosity halo mass relation of up to 1 dex, and that quasar clustering can not be used to estimate the quasar lifetime.

**Key words:** cosmology: large scale structure, theory – quasars: general

## 1 INTRODUCTION

The Sloan Digital Sky Survey (SDSS; York et al. 2000) and the 2dF quasar redshift survey (Croom et al. 2001a) have measured redshifts for large samples of quasars, and determined their luminosity function over a broad section of cosmic history (Boyle et al. 2000; Richards et al. 2006). These surveys have also been used to constrain the clustering properties of quasars (e.g. Croom et al. 2001b; Croom et al. 2002; Croom et al. 2005; Porciani & Norberg 2006; da Angela et al. 2008; Padmanabhan et al. 2008), including the variation of clustering length with redshift and luminosity. In the local Universe quasars have clustering statistics similar to optically selected galaxies, with a clustering length  $R_0 \approx 8\text{Mpc}$ . The clustering length increases towards high redshift, but is only weakly dependent on luminosity. This has been interpreted as evidence for a model in which the quasar luminosity takes on a broad range of values at different stages of its evolution (Lidz et al. 2006).

In addition to the large quasar samples below  $z \sim 3$ , the Sloan Digital Sky Survey (SDSS) has discovered luminous quasars at redshifts as high as  $z \sim 6.4$ , i.e., when the universe was less than a billion years old (Fan et al. 2001a,b; Fan

et al. 2003; Fan et al. 2006). The supermassive black-holes (SMBH) powering these quasars have masses of  $\gtrsim 10^9 M_\odot$ . Recently, clustering measurements of quasars have been extended out to redshifts beyond  $z \sim 4$  using the Fifth Data release of the SDSS (Shen et al. 2007). Quasars are shown to be significantly more clustered at high redshift relative to the more local samples, with values of  $R_0 \approx 12\text{Mpc}$  and  $R_0 \approx 17\text{Mpc}$  at  $z \sim 3$  and  $z > 3.5$  respectively (Shen et al. 2007). White, Martini & Cohn (2008) have recently shown that this large clustering length can be associated with the observation of a very large clustering bias of  $b = 14.2 \pm 1.4$  for quasars at  $z \sim 4$ .

It was argued by Martini & Weinberg (2001) and Haiman & Hui (2001), that the quasar correlation length can be used to infer the typical mass of dark matter halos in which quasars reside. One may then derive the quasar duty-cycle by comparing the number density of quasars with the density of host dark matter halos. The quasar lifetime follows from the product of the duty-cycle and the time that the dark-matter halo spends in between major mergers (although there is a degeneracy between the lifetime and the quasar occupation fraction or beaming). Results from

arXiv:0810.3455v1 [astro-ph] 20 Oct 2008

low redshift clustering have suggested quasar lifetimes of  $t_q \sim 10^6\text{--}10^7$  years, consistent with the values determined by other methods (see Martini 2003 for a review). More recently, Shen et al. (2007) have applied this analysis to their measurements of quasar clustering at high redshift. They infer lifetimes of  $t_q \sim 3 \times 10^7\text{--}6 \times 10^8$  years for quasars at  $z > 3.5$ .

Using techniques similar to those employed at low redshift, this result has been used by White et al. (2008) to argue that the scatter in the relation between quasar luminosity and halo mass must be smaller than 0.3dex. This small scatter poses a problem for theories of quasar growth and formation. The tightest local relation is observed between the black hole mass and bulge velocity dispersion, also with a scatter of  $\sim 0.3$  dex. However, the relation between quasar luminosity and halo mass must have several additional sources of scatter, including in the relation between halo mass and velocity dispersion, and between black hole mass and quasar luminosity. It is therefore difficult to understand how the luminosity – halo mass relation could be as tight as the black-hole mass – velocity dispersion relation.

The conclusion of White et al. (2008) arises because an increased scatter would tend to bring large numbers of low bias halos (which are more common) into a sample of halos at fixed quasar luminosity. The required small scatter therefore depends crucially on the assumption that the value of the observed bias truly reflects the actual bias of the quasar host galaxies. However additional bias may exist beyond the usual halo bias for systems which are triggered by mergers, although the magnitude (and even the sign) of the effect are still being debated (e.g., Kolatt et al. 1999; Gottlober et al. 2002; Kauffmann & Haehnelt 2002; Percival et al. 2003; Scannapieco & Thacker 2003; Gao, Springel & White 2005; Wetzel et al. 2007). Interpreting the results of simulations of the effect of mergers on bias is complicated by the small range of redshift and mass available in different studies. Furlanetto & Kamionkowski (2006) attempted to describe the clustering bias of merging systems more generally based on an analytic model. They concluded that a peak-background split approach within the extended Press-Schechter formalism cannot be used to calculate the merger bias because the large scale density field does not enter the calculation of merger rates using this approach. Instead, Furlanetto & Kamionkowski (2006) calculated the merger bias in models where the merger rate per halo is assumed to scale with the number densities of neighboring halos. Since this model does not account for the large scale density in the merger rate itself (but only in the halo densities), Furlanetto & Kamionkowski (2006) argue that it can only be considered qualitative. However, the model suggests that merging halos are significantly more clustered than isolated halos, by a factor of  $\sim 1.5$  for massive halos at  $z \sim 3$ . Furlanetto & Kamionkowski (2006) also proposed a simple model in which close pairs are assumed to be merging systems, and compute the bias of those based on probabilities of separation based on clustering statistics in a variety of models, with similar results.

The possibility that the observed bias exceeds the average halo bias at a particular halo mass is not restricted to scenarios where observed objects are merger driven. A separate, but related issue concerns halo formation bias. Here sub-samples of dark matter halos of fixed mass and redshift

are shown to have clustering statistics that depend on their formation history (Gao, Springel & White 2005; Croton, Gao & White 2007; Wetzel et al. 2007). For example, if the existence of luminous quasars required that the host halo be older than a particular minimum age, then this sub-sample of halos would have a clustering bias in excess of the halo population as a whole.

Since luminous quasars play an important role in the evolution of massive galaxies at high redshifts, a variety of models have been proposed to explain the high redshift luminosity function of quasars (e.g. Haiman & Loeb 1998; Haehnelt, Natarajan & Rees 1998; Kauffmann & Haehnelt 2000; Volonteri, Haardt & Madau 2003; Wyithe & Loeb 2003; Di Matteo, Springel & Hernquist 2005; Hopkins & Hernquist 2008; Hopkins et al. 2008; Li et al. 2007). The majority of these models assume that major mergers drive the quasar activity, implying that the observed bias should not simply reflect the bias based on the host halo mass.

In this paper we investigate the evidence for an additional bias, beyond the spatial clustering of dark matter halos, in the clustering data of high redshift quasars. Wyithe & Padmanabhan (2006) showed that different models are able to reproduce the data on the high redshift quasar luminosity function, implying a degeneracy among their input physical parameters. For this reason, we will not attempt to model physical processes such as SMBH growth and feedback, but instead adopt the more general approach of parameterising relations like the correlation between SMBH mass and halo mass. We are interested in the full range of allowed parameters as well as in which sets of parameters can be excluded, rather than in a particular set of parameters that is able to describe the data. This approach allows us to isolate the relationships that are constrained by the data, and to provide robust observational input for future theoretical modeling. In particular, the contribution of mergers to the observed clustering bias could be large, although its value is theoretically uncertain. We therefore treat this contribution as a free parameter, and attempt to constrain its value.

In our numerical examples we adopt the standard set of cosmological parameters (Komatsu et al. 2008), with values of  $\Omega_m = 0.24$ ,  $\Omega_b = 0.046$  and  $\Omega_Q = 0.72$  for the matter, baryon, and dark energy fractional density respectively, and  $h = 0.70$ , for the dimensionless Hubble constant. We assume  $\sigma_8 = 0.82$  for the *rms* amplitude of the density field fluctuations within spheres of radius  $8h^{-1}\text{Mpc}$  linearly extrapolated to  $z = 0$ , and a power-law slope for the primordial density power-spectrum of  $n_s = 0.96$ .

## 2 MODEL

Quasars are known to have a finite distribution of Eddington ratios (Kollmeier et al. 2006),  $\eta \equiv l/L_{\text{Edd}}$ , where  $l$  and  $L_{\text{Edd}}$  are the quasar and Eddington luminosities respectively, and are thought to have a light-curve that varies across a large range of luminosity during the quasar lifetime (Hopkins & Hernquist 2008). We can express this lightcurve as  $l(t, M_{\text{bh}}) \propto \eta(t)M_{\text{bh}}$ , where  $M_{\text{bh}}$  is the black hole mass and  $\eta$  is a dimensionless function of time. Consider now a population of quasars at a fixed instant in time. We expect to observe a range of quasar luminosity  $l$  at fixed host halo

mass  $M$  because different quasars will be at a different phase of their light curve. We first compute the distribution of luminosity  $l$  at fixed halo mass and fixed black hole mass

$$\left. \frac{dP}{dl} \right|_{M, M_{\text{bh}}} \propto \frac{dt}{dl} \frac{dP_{\text{prior}}}{dt} \propto \left( M_{\text{bh}} \frac{d\eta}{dt} \right)^{-1} \frac{\Theta(t_{\text{lt}})}{t_{\text{lt}}}. \quad (1)$$

Here,  $(dP_{\text{prior}}/dt) = \Theta(t_{\text{lt}})/t_{\text{lt}}$  (where  $\Theta$  is the Heaviside Step function), is constant during the quasar lifetime ( $0 < t < t_{\text{lt}}$ ), and zero at other times. The distribution of  $l$  at fixed halo mass is then

$$\left. \frac{dP}{dl} \right|_M \propto \int dM_{\text{bh}} \left. \frac{dP}{dM_{\text{bh}}} \right|_M \left. \frac{dP}{dl} \right|_{M, M_{\text{bh}}}, \quad (2)$$

where  $\left. \frac{dP}{dM_{\text{bh}}} \right|_M$  is the probability distribution for the black-hole mass which depends on halo mass. The mean of the logarithm of the luminosity at halo mass  $M$  can now be calculated from

$$(\log L)(M) = \int d \log l \log l \left. \frac{dP}{d \log l} \right|_M, \quad (3)$$

while the variance (in dex) can be calculated as

$$\Delta^2(M) = \int d \log l (\log l - \log L)^2 \left. \frac{dP}{d \log l} \right|_M. \quad (4)$$

In this paper we do not use the above equations to compute the relation between the quasar luminosity,  $L$ , and host halo mass,  $M$ . Rather, we suggest a parametrised form based on the above definitions and constrain the parameters of the  $L$ - $M$  relation using the available data for high redshift quasars. We begin by parameterising the relation between the mean quasar luminosity,  $L$ , and host halo mass,  $M$ , as

$$\frac{L}{L_0} = \left( \frac{M}{M_0} \right)^\gamma, \quad (5)$$

where  $L_0$  and  $M_0$  are normalisation constants. We then suppose that this relation has an intrinsic scatter in luminosity  $l$  at fixed halo mass  $M$  of  $\Delta$ . For simplicity, we assume that the distribution  $dP/dl|_M$  is log-normal and express its scatter in dex. Re-writing the mean relation as

$$M = M_0 \left( \frac{L}{L_0} \right)^{\frac{1}{\gamma}}, \quad (6)$$

we then specify the scatter in the  $M$ - $L$  relation in terms of a probability distribution for halo mass  $m$  at fixed luminosity  $L$  i.e.

$$\left. \frac{dP}{d \log m} \right|_L = \frac{1}{\sqrt{2\pi}(\Delta/\gamma)} \exp \left[ \frac{(\log m - \log M)^2}{2(\Delta/\gamma)^2} \right]. \quad (7)$$

We next specify a model for the luminosity function of quasars (i.e. the number density of quasars per unit luminosity with luminosity  $L$ )

$$\frac{dn}{dL} = \int d \log m \frac{dn}{dm} \frac{dm}{dL} \Big|_{L, M_0} \left. \frac{dP}{d \log m} \right|_L f_{\text{duty}} \left( \frac{L}{L_0} \right)^\alpha, \quad (8)$$

where  $\frac{dn}{dM}$  is the Sheth-Tormen (1999) mass-function for dark matter halos of mass  $M$ , and the derivative

$$\frac{dm}{dL} = \frac{dM}{dL} \frac{dm}{dM} = \frac{m}{M} \frac{M_0}{L_0} \frac{1}{\gamma} \left( \frac{L}{L_0} \right)^{\frac{1}{\gamma}-1}. \quad (9)$$

The duty-cycle  $f_{\text{duty}} = t_{\text{lt}}/t_H$ , where  $t_H$  is the Hubble time

at redshift  $z$ , is the fraction of halos that have a quasar in a luminous phase, and the last factor in equation (8) accounts for the possibility that the quasar lifetime  $t_{\text{lt}}$  is dependent on black hole mass<sup>1</sup>. The luminosity function has an associated logarithmic slope

$$\beta(L) \equiv \frac{d}{d \log L} \left( \log \frac{dn}{dL} \right). \quad (10)$$

We also compute the density of quasars above a limiting luminosity  $L$ ,

$$n(> L) = \int_L^\infty dL' \frac{dn}{dL'}. \quad (11)$$

The halo bias of quasars with luminosity  $L$  is given by,

$$\bar{b}(L) = \frac{\int d \log m b(m) \frac{dn}{dm} \left. \frac{dP}{d \log m} \right|_L}{\int d \log m \frac{dn}{dm} \left. \frac{dP}{d \log m} \right|_L}, \quad (12)$$

where  $b(m)$  is the halo bias of a halo with mass  $m$ , which is computed using the fitting formula of Sheth, Mo & Tormen (1999). This bias can be used to calculate the halo bias of a sample of quasars with luminosities above a limiting value.

$$\langle b \rangle = \frac{\int_L^\infty dL' \bar{b}(L') \frac{dn}{dL'}}{\int_L^\infty dL' \frac{dn}{dL'}}. \quad (13)$$

As noted in §1, this average halo bias may underestimate the observed quasar bias if quasars are triggered by galaxy mergers (Furlanetto & Kamionkowski 2006). To account for this possibility, we introduce a free parameter  $F$ , defined as the ratio of the observed bias  $b_{\text{obs}}$  to the halo bias  $\langle b \rangle$ ,

$$F \equiv \frac{b_{\text{obs}}}{\langle b \rangle}. \quad (14)$$

Note that the value of the black-hole mass does not enter our calculations. Thus, our conclusions are insensitive to assumptions regarding the Eddington ratio and the relation between black-hole mass and halo mass. Conversely, this means that our model is not able to address issues surrounding these relations. Nevertheless, as we show below, this simplicity does allow our model to reach some strong conclusions regarding the relationship between the observed quasar clustering and the host halo mass.

Before proceeding to analyse the implications of existing observational data, we note that the detailed results are sensitive to the form of the halo mass function. Our fiducial calculations use the Sheth-Tormen form. However in § 3.5 we also present results using the corresponding Press-Schechter formulation to assess the level of theoretical uncertainty in the results.

<sup>1</sup> In this paper we only consider the luminosity function and its slope at a single value of luminosity. While we have quoted a power-law form for the dependence of duty cycle on luminosity we note that this should be thought of as a logarithmic slope at luminosity  $L$ . In general the value of  $\alpha$  must be luminosity dependent or else the duty-cycle would exceed unity for some values of luminosity.

### 3 COMPARISON WITH OBSERVATIONS

The quantities  $n(> L)$ ,  $\beta$  and  $b_{\text{obs}}$  are observed properties of the quasar population, with values of  $n(> L) \sim 0.7 \times 10^{-7} \text{Mpc}^{-1}$ ,  $\beta = -2.58 \pm 0.23$  and  $b_{\text{obs}} = 14.2 \pm 1.4$ , respectively. The quasar sample from which the clustering and corresponding density data were obtained was described in Shen et al. (2007). The bias and density for quasars at  $z \sim 4$  were discussed for this sample in White, Martini & Cohn (2008), and we use their calculated bias in this paper. The luminosity function slope is taken from the quasar luminosity function analysis of Fan et al. (2001b), for which the mean quasar redshift and absolute AB magnitude at  $1450\text{\AA}$  were  $z = 4.3$  and  $M_{1450} \approx -26$ , respectively. These quantities can be compared to the theoretical expectations described above, and hence used to constrain the free parameters,  $f_{\text{duty}}$ ,  $\alpha$ ,  $\Delta$ ,  $\gamma$  and  $F$ .

#### 3.1 Results

We begin by illustrating the dependencies of the observables on the available free parameters. In Figures 1 and 2 we show contours of constant  $\langle b \rangle / F$  in the plane of  $f_{\text{duty}}$  and  $\Delta$ . Since the halo bias is related to the observed bias through an unknown constant  $F$ , we begin by showing two cases for illustration. In the first we choose  $F = 1$ , which is the standard model employed to link clustering statistics to halo mass and quasar lifetime in previous studies (Martini & Weinberg 2001; Haiman & Hui 2001; White, Martini & Cohn 2008). In the second, we adopt  $F = 1.5$ , which is approximately the factor by which the observed bias exceeds the halo bias in the models of Furlanetto & Kamionkowski (2006). In Figures 1 and 2 the solid and dashed contours are plotted for values of  $F = 1.0$  and  $F = 1.5$ , respectively. We find that there are no combinations of  $f_{\text{duty}}$  and  $\Delta$  that produce the best fit value of the observed bias for  $F = 1$  (see also White, Martini & Cohn 2008). In this case we draw a contour (solid line) at the  $2\text{-}\sigma$  lower limit of  $\langle b \rangle = (14.2 \pm 1.4) / F = 14.2 - 2.8 = 11.4$ . In the second case with  $F = 1.5$ , the contours (dashed lines) are drawn to correspond to the observed bias  $\langle b \rangle = (14.2 \pm 1.4) / F$ .

In constructing these contours, for each combination of  $f_{\text{duty}}$  and  $\Delta$  the luminosity  $L$  is chosen so that the luminosity function reproduces the observed density of quasars. The duty cycle on the  $x$ -axis corresponds to quasars with this luminosity  $L$ . For fixed values of  $F$ ,  $\gamma$  and  $\alpha$ , the contours in Figures 1 and 2 enclose the acceptable combinations of  $f_{\text{duty}}$  and  $\Delta$ , given the constraint of the observed bias. We find that smaller values of duty-cycle permit smaller values of intrinsic scatter in the  $L - M$  relation. The two figures separate the effect of the parameters  $\alpha$  and  $\gamma$  on the derived constraints. In Figure 1 we set  $\alpha = 0$  and vary the value of  $\gamma$ . In Figure 2, we fix the value of  $\gamma = 1$  and vary  $\alpha$ . The observed bias tightly constrains the scatter in the  $L - M$  relation (White et al. 2008). In particular, if  $F = 1$ ,  $\gamma = 1$ , the constraints show that  $\Delta < 0.1$  at the  $2\text{-}\sigma$  level, which is tighter than the local relation between black-hole mass and velocity dispersion. The clustering and density data are not consistent with  $F = 1$  at the  $1\text{-}\sigma$  level for any of the parameter sets shown. Since the scatter  $\Delta$  must be finite, the contours therefore suggest that  $F > 1$ , even at the highest possible duty-cycle.

In addition to the observed bias, our model is constrained by the observed luminosity function slope. In Figures 1 and 2 we also show the region of parameter space that is consistent with the constraint from the observed luminosity function slope (grey scale). The predicted slope is sensitive to the value of  $\gamma$ . As a result, the values of  $f_{\text{duty}}$  and  $\Delta$  that are consistent with the observed slope are also sensitive to  $\gamma$ . Viable models must have overlapping regions of parameter space that satisfy the different constraints. Figures 1-2 show that unless  $\gamma$  or  $\alpha$  are large, there are no combinations of  $f_{\text{duty}}$  and  $\Delta$  that are even marginally consistent with the constraints of observed bias and luminosity function slope for  $F = 1$ .

#### 3.2 Joint Likelihood distributions for pairs of parameters

To quantify the above conclusions we next calculate the joint likelihoods for pairs of parameters, and the a posteriori probability distributions for individual parameters.

The likelihood for the parameter set  $(\Delta, \gamma, f_{\text{duty}}, F, \alpha)$  is

$$\mathcal{L}_{\Delta, \gamma, f_{\text{duty}}, F, \alpha} = \exp \left( -\frac{1}{2} \left[ \left( \frac{F \langle b \rangle - 14.2}{1.4} \right)^2 + \left( \frac{\beta - 2.58}{0.23} \right)^2 \right] \right). \quad (15)$$

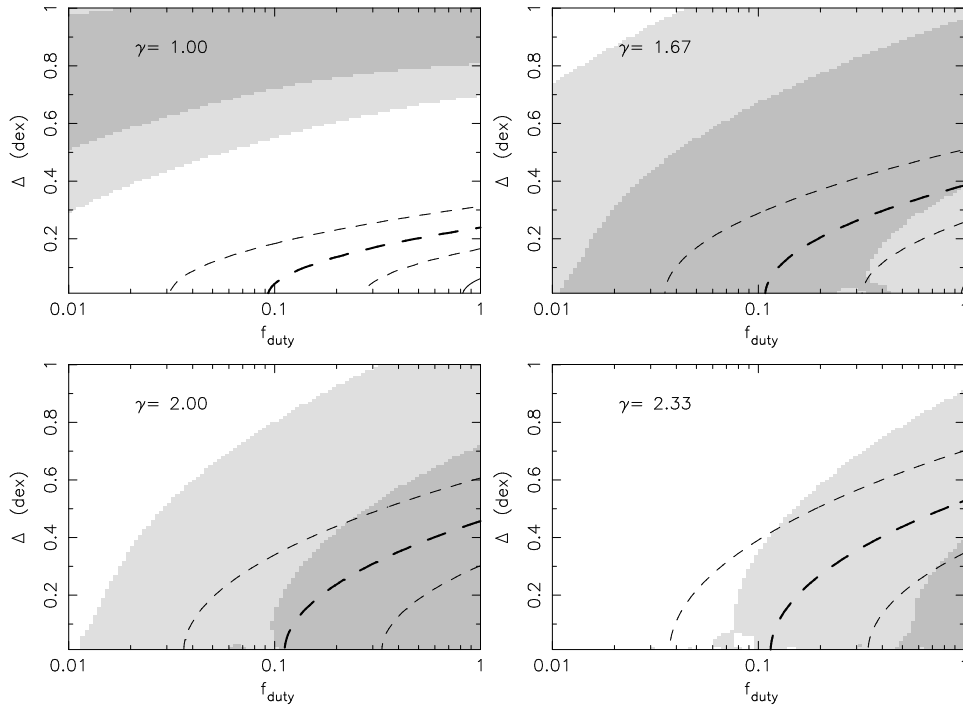
We then obtain marginalised likelihoods by integrating over the remaining parameters. For example, the joint likelihood for  $\Delta$  and  $f_{\text{duty}}$  is

$$\mathcal{L}_{\Delta, f_{\text{duty}}} \propto \int_{\alpha_{\text{min}}}^{\alpha_{\text{max}}} d\alpha \int_{\gamma_{\text{min}}}^{\gamma_{\text{max}}} d\gamma \int_{F_{\text{min}}}^{F_{\text{max}}} dF \mathcal{L}_{\Delta, \gamma, f_{\text{duty}}, F, \alpha} \times \frac{dP_{\text{prior}}}{d\alpha} \frac{dP_{\text{prior}}}{d\gamma} \frac{dP_{\text{prior}}}{dF}, \quad (16)$$

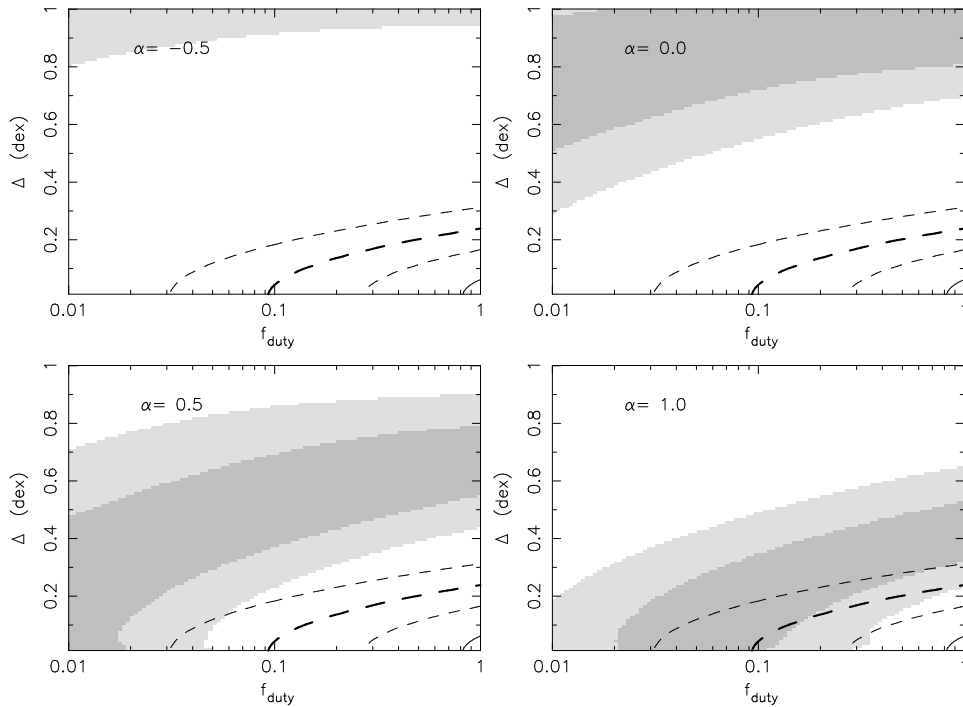
where  $\alpha_{\text{min}}$  and  $\alpha_{\text{max}}$  are the bounding values on the finite region of the prior probability distribution  $dP_{\text{prior}}/d\alpha$  for the variable  $\alpha$ , and so on. We assume constant prior probability distributions for  $\alpha$ ,  $\Delta$  and  $\gamma$ . For  $F$  and  $t_{\text{duty}}$ , which are fractional quantities, we assume prior probability distributions that are flat in the logarithm of these quantities. We assume the prior probability to be non-zero within the following ranges:  $\alpha_{\text{min}} = -2$ ,  $\alpha_{\text{max}} = 2$ ;  $\gamma_{\text{min}} = 0$ ,  $\gamma_{\text{max}} = 2.5$ ;  $\Delta_{\text{min}} = 0$ ,  $\Delta_{\text{max}} = 2$ ;  $F_{\text{min}} = 0.5$ ,  $F_{\text{max}} = 3$ ;  $f_{\text{duty, min}} = 0.01$ ,  $f_{\text{duty, max}} = 1$ . While some of our quantitative results are sensitive to the values of these limits, our primary qualitative conclusions are robust to the choice of the prior probability distributions and their ranges.

Figure 3 shows contours of the joint likelihood distributions for  $f_{\text{duty}}$  and  $F$  (top left panel), for  $\gamma$  and  $F$  (top right panel), for  $\Delta$  and  $\alpha$  (central left panel), for  $F$  and  $\Delta$  (central right panel), for  $F$  and  $\alpha$  (lower left panel) and for  $\gamma$  and  $\alpha$  (lower right panel). Contours are shown at 60% and 7% of the maximum likelihood. Since the number of free parameters exceeds the number of observables, a unique model cannot be found. Nevertheless, the results of Figure 3 illustrate that despite some degeneracies, several interesting statements can be made regarding the allowed parameter values.

Our main results are as follows. First, the parameter  $\alpha$  is constrained to lie within a finite range centered around  $\alpha \approx -0.3$ . In addition, lower limits can be placed on the



**Figure 1.** *Solid and dashed lines:* Contours of joint likelihood for pairs of  $\Delta$  and  $f_{\text{duty}}$  given the observed bias. The solid and dashed contours correspond to values of  $F = 1.0$  and  $F = 1.5$ , respectively. For  $F = 1$ , the contour is drawn at the  $2\text{-}\sigma$  lower limit of  $\langle b \rangle = 11.4$ . For  $F = 1.5$ , the contours are drawn at  $\langle b \rangle = (14.2 \pm 1.4)/F$ . In each case the luminosity  $L$  corresponds to the observed density of quasars. The grey-scale shows the corresponding joint likelihood given the constraint of the observed luminosity function slope  $\beta = -2.58 \pm 0.23$ . The dark and light grey show the regions where the predicted slope is within 1 and 2-sigma of the best fit value. Four examples are shown for different values of  $\gamma$ , with  $\alpha = 0$  in all cases.



**Figure 2.** As per Figure 1, but for different values of  $\alpha$ , with  $\gamma = 1$  in each case.

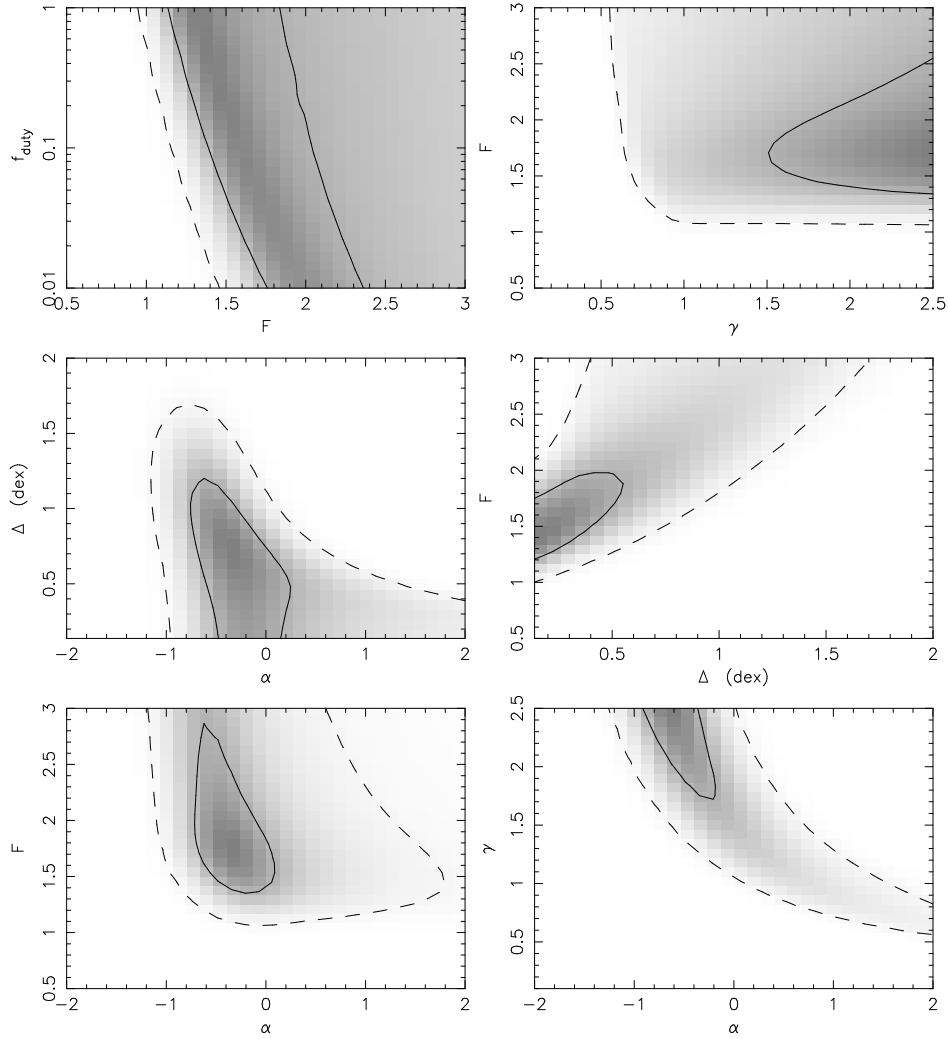


**Figure 3.** Contours of the joint likelihood distributions for  $f_{\text{duty}}$  and  $F$  (top left panel), for  $\gamma$  and  $F$  (top right panel), for  $\Delta$  and  $\alpha$  (central left panel), for  $F$  and  $\Delta$  (central right panel), for  $F$  and  $\alpha$  (lower left panel) and for  $\gamma$  and  $\alpha$  (lower right panel). Contours are shown at 60% (solid) and 7% (dotted) of the maximum likelihood. See text for details on the assumed prior probability distributions.

value  $\gamma$ , which we find to be larger than unity. The value of the scatter is restricted to be  $\Delta \lesssim 1$  dex. This constraint is much less stringent than the conclusion of White, Martini & Cohn (2008). The difference can be traced to the fact that White et al. (2008) assumed the halo bias to be equal to the observed bias. We find that degeneracies prevent the data from imposing an upper limit on  $\gamma$  or a lower limit<sup>2</sup> on  $\Delta$  (although the latter cannot be negative). We find that the duty cycle is unconstrained by these observations. This result differs from previous studies (e.g. Martini & Weinberg 2001) because the parameter  $F$  removes the direct connection between halo bias and halo mass (and hence halo density). The value of  $F$  is constrained to be larger than unity. This is our most important conclusion, and we will return to its implications in § 4.

<sup>2</sup> Note that the value of  $\Delta$  would be expected lie in excess of the scatter of  $\sim 0.3$  dex in the local relation between velocity dispersion and black-hole mass. Inclusion of this constraint as a prior on  $\Delta$  tightens the constraints on other parameters but does not change our qualitative conclusions.

### 3.3 Constraints on individual parameters

By analogy with equation (16), the joint likelihood function  $\mathcal{L}_{\Delta, \gamma, f_{\text{duty}}, F, \alpha}$  can be marginalised over all remaining parameters to find the likelihood for a single variable. For example, the likelihood for  $\Delta$  is

$$\mathcal{L}_{\Delta} \propto \int_{f_{\text{duty}, \text{min}}}^{f_{\text{duty}, \text{max}}} df_{\text{duty}} \int_{\alpha_{\text{min}}}^{\alpha_{\text{max}}} d\alpha \int_{\gamma_{\text{min}}}^{\gamma_{\text{max}}} d\gamma \int_{F_{\text{min}}}^{F_{\text{max}}} dF \mathcal{L}_{\Delta, \gamma, f_{\text{duty}}, F, \alpha} \frac{dP_{\text{prior}}}{d\alpha} \frac{dP_{\text{prior}}}{df_{\text{duty}}} \frac{dP_{\text{prior}}}{d\gamma} \frac{dP_{\text{prior}}}{dF}. \quad (17)$$

The a posteriori probability density for  $\Delta$  becomes

$$\frac{dP}{d\Delta} \propto \mathcal{L}_{\Delta} \frac{dP_{\text{prior}}}{d\Delta},$$

with the normalisation,

$$\int_{\Delta_{\text{min}}}^{\Delta_{\text{max}}} \frac{dP}{d\Delta} d\Delta = 1.$$

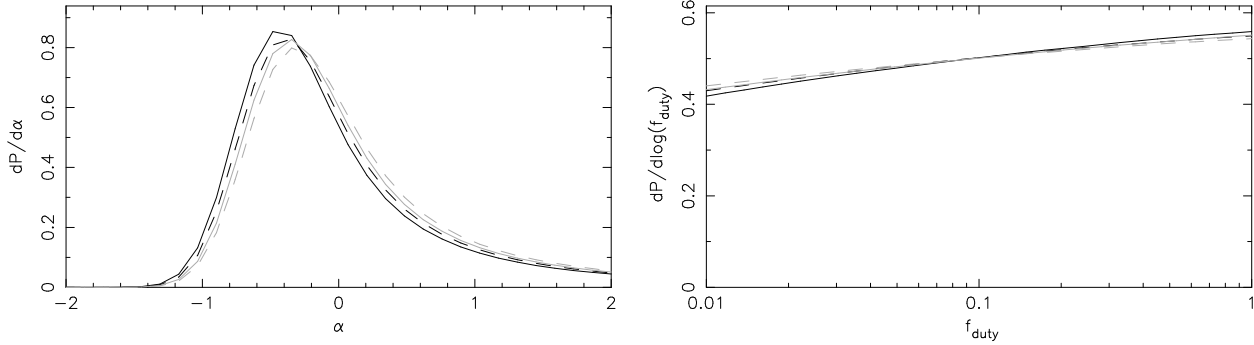


**Figure 4.** Marginalised, a' posteriori differential probability distributions for  $\alpha$  (left) and  $f_{\text{duty}}$  (right). The black and grey lines correspond to calculations performed using the Press-Schechter and Sheth-Tormen formalisms respectively. The solid (dashed) lines do (do not) include the correction factor of 2 in the quasar density (see text for details).

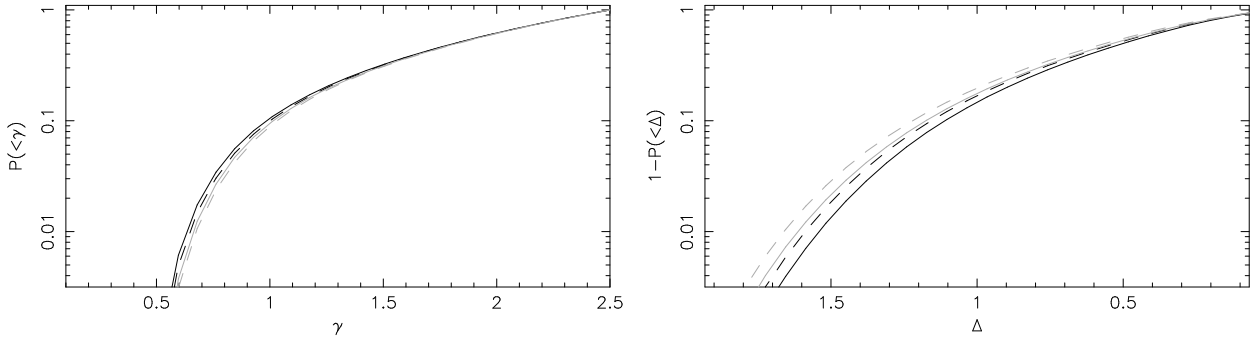


**Figure 5.** Marginalised, a' posteriori cumulative probability distributions for  $\gamma$  (left) and  $\Delta$  (right). The black and grey lines correspond to calculations performed using the Press-Schechter and Sheth-Tormen formalisms respectively. The solid (dashed) lines do (do not) include the correction factor of 2 in the quasar density.

The corresponding a' posteriori cumulative probability is

$$P(< \Delta) = \int_{\Delta_{\text{min}}}^{\Delta} d\Delta' \frac{dP}{d\Delta'}.$$

Figure 4 shows the differential distributions  $dP/d\alpha$  and  $dP/df_{\text{duty}}$ . The data constrains a value of  $\alpha \approx -0.4 \pm 0.5$ , while the value of  $f_{\text{duty}}$  remains unconstrained. The left-hand panel of Figure 5 shows the cumulative distribution for  $\gamma$ . This distribution shows that  $\gamma$  must be greater than unity at a statistical confidence of 90%. Similarly, the right-hand panel shows the value of 1 minus the cumulative probability distribution for  $\Delta$ . At 90% confidence, the scatter can only be shown to be below  $\Delta = 1.1$  (in difference from White et al. 2008). Finally, Figure 6 plots the differential (left,  $dP/dF$ ) and cumulative [right,  $P(< F)$ ] distributions for  $F$ . The most likely value is at  $F \approx 1.7$ . The probability drops rapidly towards low values of  $F$  and we find that  $F > 1.1$  with high statistical confidence (99%).

As noted above, our quantitative results are sensitive to the prior probability distributions because the number of free parameters is larger than the number of constraints. In particular, we find that the data does not constrain the upper limit of the parameters  $\gamma$  or  $F$ . As a result, our quantitative results are sensitive to the values chosen for the parameters of  $\gamma_{\text{max}}$  and  $F_{\text{max}}$ . However, if we increase the values of  $\gamma_{\text{max}}$  and  $F_{\text{max}}$ , permitting a greater volume of parameter space a' priori, then our constraints on the lower limits for  $\gamma$  and  $F$  are improved. Therefore, our qualitative con-

clusions are not sensitive to the assumed prior probability distribution. In summary, we find constraints on individual parameters of  $\alpha \approx -0.4 \pm 0.5$ ,  $\gamma > 1$  (at a statistical confidence of 90%),  $\Delta < 1.1$  (90%) and  $F > 1.1$  (99%).

### 3.4 Constraints on host halo mass

Finally, we are able to use the above constraints to assess the range of halo masses that are consistent with the clustering and luminosity function data. In our formalism the halo mass is not a free parameter. Rather, for each parameter set  $\Delta, \gamma, f_{\text{duty}}, F, \alpha$ , there is a halo mass  $M_{\Delta, \gamma, f_{\text{duty}}, F, \alpha}$ , which corresponds to the observed quasar density. Since our formalism includes scatter in the  $L-M$  relationship, this mass is defined as the mean mass  $M$  at luminosity  $L$  (equation 6). This parameter combination has likelihood  $\mathcal{L}_{\Delta, \gamma, f_{\text{duty}}, F, \alpha}$ . The probability distribution for  $M$  can therefore be computed from

$$\begin{aligned} \frac{dP}{dM} &\propto \\ &\int_{\Delta_{\text{min}}}^{\Delta_{\text{max}}} d\Delta \int_{f_{\text{duty}, \text{min}}}^{f_{\text{duty}, \text{max}}} df_{\text{duty}} \int_{\alpha_{\text{min}}}^{\alpha_{\text{max}}} d\alpha \int_{\gamma_{\text{min}}}^{\gamma_{\text{max}}} d\gamma \int_{F_{\text{min}}}^{F_{\text{max}}} dF \\ &\mathcal{L}_{\Delta, \gamma, f_{\text{duty}}, F, \alpha} \frac{dP_{\text{prior}}}{d\Delta} \frac{dP_{\text{prior}}}{df_{\text{duty}}} \frac{dP_{\text{prior}}}{d\alpha} \frac{dP_{\text{prior}}}{d\gamma} \frac{dP_{\text{prior}}}{dF} \\ &\times \delta(M - M_{\Delta, \gamma, f_{\text{duty}}, F, \alpha}), \end{aligned} \quad (18)$$

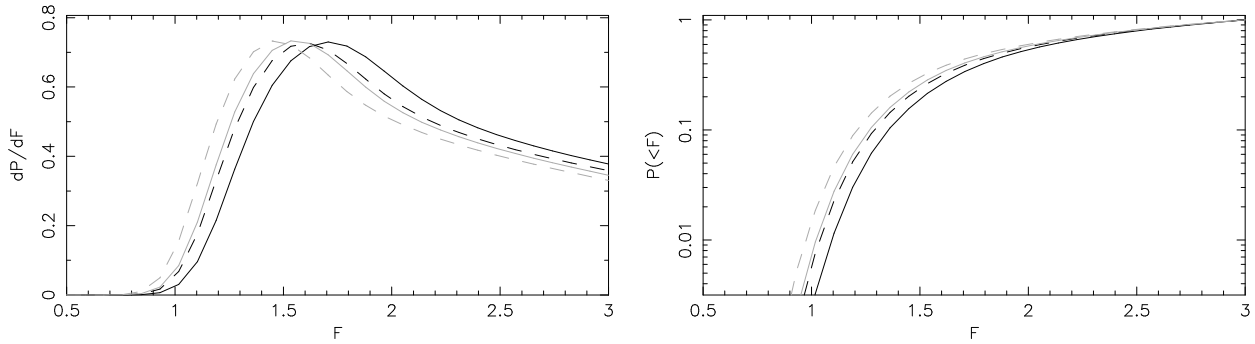


**Figure 6.** Marginalised, a'posteriori differential (left) and cumulative (right) probability distributions for  $F$ . The black and grey lines correspond to calculations performed using the Press-Schechter and Sheth-Tormen formalisms respectively. The solid (dashed) lines do (do not) include the correction factor of 2 in the quasar density.

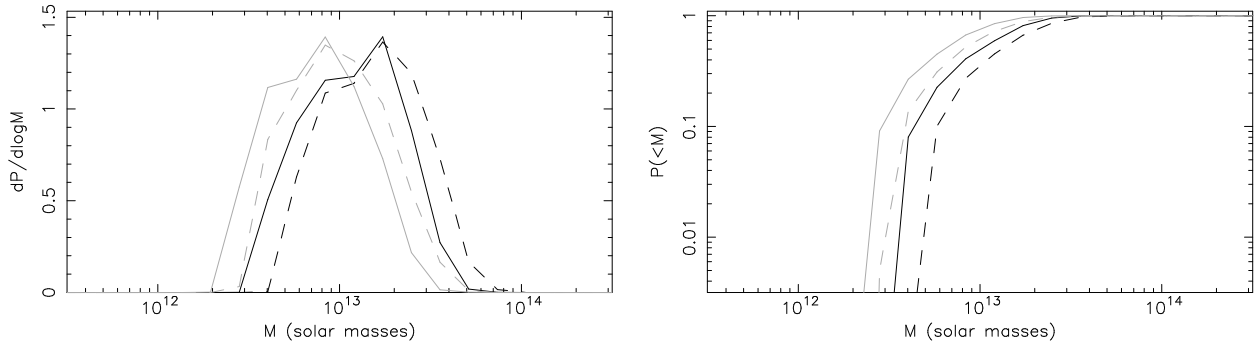


**Figure 7.** Marginalised, a'posteriori differential (left) and cumulative (right) probability distributions for halo mass  $M$ . The black and grey lines correspond to calculations performed using the Press-Schechter and Sheth-Tormen formalisms respectively. The solid (dashed) lines do (do not) include the correction factor of 2 in the quasar density.

with corresponding cumulative distribution

$$P(< M) = \int_M^\infty dM' \frac{dP}{dM'}. \quad (19)$$

We plot these distributions in Figure 7. The host halo mass for the quasars in the high redshift sample is  $M \sim 10^{13 \pm 0.5} M_\odot$ . In our fiducial model, the halo mass is restricted to be larger than  $\sim 3 \times 10^{12} M_\odot$  (99%). This mass range is comparable to the one ( $M \gtrsim 5 \times 10^{12} M_\odot$ ) quoted by Shen et al. (2007). However, note that here  $M$  refers to the halo mass corresponding to  $L$  at the mean of the  $L$ - $M$  relation. The possibility of a large intrinsic scatter means that many host halos will have a significantly smaller mass.

### 3.5 Theoretical uncertainties in the bias

Thus far we have presented a fiducial model using the Sheth-Tormen forms for the clustering bias (Sheth, Mo & Tormen 1999) and the mass-function (Sheth & Tormen 1999). However as demonstrated in White, Martini & Cohn (2008), the bias and density are sufficiently large as to make any quantitative conclusions sensitive to the detailed predictions of the Sheth-Tormen model. A discussion of the various analytic models and their comparison to numerical simulation is provided by White, Martini & Cohn (2008), who suggest that the Press-Schechter and Sheth-Tormen formalisms should bracket the expected level of theoretical uncertainty. Following this assertion, we also present results

using the corresponding Press-Schechter formulation for the mass function (Press-Schechter 1974) and clustering bias (Mo & White 1996) to assess the level of theoretical systematic uncertainty in our conclusions.

In addition to the adopted model for the statistics of the halo population, the conclusions will also be sensitive to the value of the measured space density of quasars. Shen et al. (2007) pointed out that the space density is underestimated by a factor of  $\sim 2$  for the fit of Richards et al. (2006). Following White, Martini & Cohn (2008) we have used that correction factor in our analysis above. For comparison, we also repeat our analysis using the uncorrected value of  $N = 0.35 \times 10^{-7} \text{Mpc}^{-3}$ .

We therefore compare a set of four calculations, using combinations of the Sheth-Tormen or Press-Schechter halo statistics with the quasar density computed with or without the correction factor. In Figures 4-7 we show probability distributions for the three additional cases together with our fiducial model. The constraints on  $\gamma$  and  $\alpha$  are unaffected by these model changes since these are not directly related to the numbers of observed quasars. The lower density of quasars and the larger predicted bias of the Press-Schechter formalism (and their combination) each yield weaker constraints on  $\Delta$ ,  $F$  than our fiducial model. However the systematic effect is mild, with limits of  $\Delta < 1.1$  (85%), and  $F > 1.1$  (98%). We find that the minimum halo mass is effected by a factor of 2 depending on the assumed combination.

#### 4 DISCUSSION

We find that the value of  $F$  is constrained to be in excess of unity, i.e. the observed bias is in excess of the halo bias. This could be interpreted as evidence that mergers are responsible for the quasar activity. We also find that  $\gamma > 1$ , implying that the luminosity to halo mass ratio increases with halo mass. Under the assumption that the Eddington ratio of bright quasars is nearly constant (as argued by Kollmeier et al. 2006), models of feedback limited growth through energy deposition (Haehnelt, Nataraajan & Rees 1998; Wyithe & Loeb 2003) predict a value of  $\gamma = 5/3$ . If we adopt  $\gamma = 5/3$ , then the preferred range of  $F$  (marginalised over other parameters) is  $1.5 \lesssim F \lesssim 2$ . Interestingly,  $F \sim 1.5$  is approximately the factor by which Furlanetto & Kamionkowski (2006) estimated mergers to increase the observed bias over the value of halo bias at high values of  $M$ . In our analysis we have allowed  $F$  to be a free parameter. This approach has the promise of constraining the merger process responsible for the triggering of quasar activity. For example, Furlanetto & Kamionkowski (2006) demonstrated that if close pairs lead to mergers, then mergers are expected to be clustered differently than individual halos. The magnitude of this difference is dependent on the clustering model, and so its measurement will constrain fundamental properties of the merger process.

Several anomalies have been previously noticed in the unexpectedly high clustering of systems that may be merger driven. For example, the clustering amplitude of Lyman-break galaxies (Adelberger et al. 2005) implies a host halo mass of  $\sim 10^{12} M_\odot$ . However at this mass, the density of Lyman-break galaxies then implies that the duty-cycle of vigorous star formation must be unity in all halos. Moreover, kinematic measurements of these galaxies imply a significantly smaller mass of  $\sim 10^{11} M_\odot$  (Pettini et al. 2001; Erb et al. 2003). The tension between the different estimates of host mass could be alleviated if the intense star formation in Lyman-break galaxies is triggered by mergers, and if mergers in turn increase the observed bias (Furlanetto & Kamionkowski 2006). In a recent paper, Wake et al. (2008) demonstrated that a radio-loud sub-sample of Luminous Red Galaxies at  $z \sim 0.55$  had a clustering amplitude that is in excess of the radio-quiete sub-sample, despite the optical properties being identical. Wake et al. (2008) interpret this as a larger host halo mass for radio loud objects. However, it might also be appealing to assign the excess bias to a merger origin of accretion activity.

Of course there are alternative explanations for each of these observations. For example, dynamical measurements may only be accessing the central component of the host halos of Lyman break galaxies (Cooray 2005). In the case of radio loud Luminous Red Galaxies, the high bias could originate from the high bias of X-ray clusters (more massive halos), of which the Luminous Red Galaxies would be the central member. Additionally, since clustering statistics have been shown to depend on the halo formation history (Gao, Springel & White 2005; Croton, Gao & White 2007; Wetzel et al. 2007), the age or structural properties the galaxy host could also effect the observed clustering. However in each case it is clear that the possibility of modification of the observed bias should be taken into account in interpreting

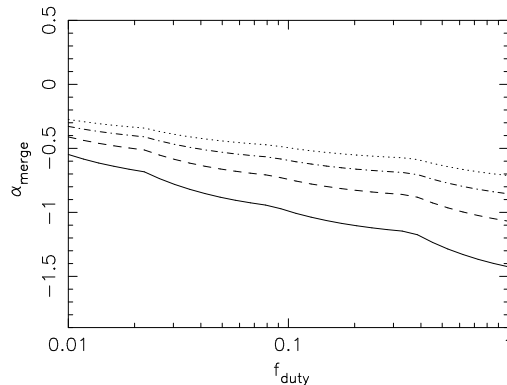


**Figure 8.** The theoretically expected value of  $\alpha_{\text{merge}}$  as a function of quasar duty cycle (see text for details). Curves are plotted for four values of  $\gamma = 1, 4/3, 5/3$ , and 2 (bottom to top).

clustering data for many types of galaxies, such as starburst galaxies or radio galaxies.

The value of  $\alpha$  is also well constrained. Since the constraint of  $F > 1$  may suggest that quasar activity is triggered by mergers, it is interesting to calculate the predicted value of  $\alpha$  using a model where the total duty cycle (i.e. summing over all quasar episodes in a single host) as a function of luminosity is proportional to the rate of major mergers. We use the extended Press-Schechter formalism to evaluate the rate of mergers of halos with mass  $M_1$  per unit mass with halos of mass  $M_2$ ,  $d^2 N/dM_1 dt|_{M_2}$  (Lacey & Cole 1993). The duty-cycle is then proportional to  $M_1 d^2 N/dM_1 dt|_{M_2} t_{\text{lt}} H$ , where  $t_{\text{lt}}$  is the lifetime of a single merger driven quasar episode and  $H^{-1}$  is the Hubble time at the redshift of interest (Wyithe & Loeb 2003). Assuming that  $t_{\text{lt}}$  is not a function of mass (as expected if the quasar episode is related to timescales like the black-hole doubling time or the dynamical time of its host galaxy), we find

$$\alpha_{\text{merge}} \approx \frac{1}{\gamma} \frac{d}{d \log M} \left[ \log \left( M \frac{d^2 N}{dM dt} \Big|_M \right) \right], \quad (20)$$

where we have assumed major mergers with  $M_1 \sim M_2 = M$ , and the term  $1/\gamma$  originates in the conversion from  $d \log M$  to  $d \log L$  for consistency with the definition of  $\alpha$ . The resulting value of  $\alpha_{\text{merge}}$  as a function of duty cycle is plotted in Figure 8 for four values of  $\gamma = 1, 4/3, 5/3$ , and 2 (bottom to top). While a value of  $\gamma = 5/3$  applies to feedback through energy deposition, models where the quasar drives the gas outflow from its host galaxy through momentum deposition have  $\gamma = 4/3$  (e.g. Silk & Rees 1998; Murray, Quataert & Thompson 2005; King 2003). Here, the value of  $\alpha_{\text{merge}}$  has been computed at a halo mass for which the number density times the duty cycle is equal to the observed quasar density. We find that for this model we would expect a value of  $-1 \lesssim \alpha_{\text{merge}} \lesssim -0.3$ , with larger values of  $\gamma$  indicating less dependence of duty cycle on luminosity. These values are consistent with our constraints on  $\alpha$ .

We note that the scatter is only constrained to satisfy  $\Delta \lesssim 1$  dex. This range is significantly larger than the tight upper limit of  $\sim 0.3$  dex found in the analysis of White et al. (2008). The difference can be traced to the greater freedom in our model associated with: (i) the relation between luminosity and halo mass through  $\gamma$ ; (ii) the relation between quasar density and halo mass through  $\alpha$ ; and (iii) the

allowance for the observed clustering bias to not directly reflect the underlying host mass for merger-driven systems. We do find that models assuming  $F = 1$ ,  $\gamma = 1$  (as considered by White, Martini & Cohn 2008) reflect the small upper limit of  $\Delta \sim 0.3$  dex. However in addition to this low value of scatter being disfavoured in our more general model by the joint constraints from clustering and luminosity function, we would not expect such a tight relationship on observational grounds. In particular, an upper limit of 0.3 dex implies a scatter that is smaller than the scatter in the black hole–velocity dispersion relation measured locally ( $\sim 0.3$  dex; Tremaine et al. 2002). However the relation between quasar luminosity and halo mass must have several additional sources of scatter, including in the relation between halo mass and bulge velocity dispersion, and between black hole mass and quasar luminosity. Hopkins et al. (2007) have investigated the scatter in relations between black-hole mass and galaxy properties including the bulge velocity dispersion. They argue that the tightness of these relations implies that any connection between black-hole mass and halo mass must be incidental. Wyithe & Loeb (2005) have modeled the black-hole – halo mass relation, and have shown that the scatter in the black-hole velocity dispersion relation combined with the statistical properties of dark-matter halos (Bullock et al. 2001) implies a scatter of at least 0.5 dex at the redshifts of interest. Moreover, any relation between luminosity and halo mass must also include a factor to account for the fraction of the Eddington rate at which the quasar accretes. Kollmeier et al. (2006) found a scatter in this distribution of 0.3dex.

Finally, we note that the quasar duty-cycle is not constrained in this model. This is in difference to previous results (Haiman & Hui 2001; Martini & Weinberg 2001; Shen et al 2007; White et al. 2008), which have constrained the quasar lifetime from clustering. The difference originates from the fact that our model does not assume the one to one correspondence between observed clustering amplitude and halo mass ( $F = 1$ ). This generalisation, motivated by the theoretical expectation that merging systems are likely to be more clustered than their isolated counterparts at fixed halo mass, means that a large clustering amplitude can be obtained by more common, lower mass halos, allowing the observed density to be achieved with a smaller duty-cycle. Moreover, Figure 3 demonstrates that even if a value of  $F \sim 1.5$  (Furlanetto & Kamionkowski 2006) is adopted, the duty-cycle still remains unconstrained. This is because the large value of  $F$  allows for reproduction of the data over a wide range of possible values for the scatter ( $\Delta$ ), which in turn allows the model to predict a broad range of values for the halo abundance.

In our analysis we have included the slope of the quasar luminosity function as an additional constraint to the quasar density and clustering. Before concluding we note that the addition of this constraint does not effect quantitative conclusions regarding  $F$  or  $\Delta$ , which are derived from comparison of the halo number density and bias to the observed density and bias. We have repeated our analysis without the constraint on the luminosity function slope. We find that the addition of this constraint allows a limit to be placed on  $\alpha$  and tightens the constraint on  $\gamma$ .

## 5 CONCLUSION

The large amplitude of the observed clustering among  $z \sim 4$  quasars, combined with their density and luminosity function slope, strongly constrains the relationship between quasar luminosity and halo mass at high redshifts. We have modelled these observables using the extended Press-Schechter formalism, combined with a mean quasar luminosity ( $L$ ) – halo mass ( $M$ ) relation of the form  $L \propto M^\gamma$ . We assume an intrinsic scatter (in dex) around the mean relation of  $\Delta$  at a fixed halo mass. We find that the observed clustering amplitude and luminosity function slope cannot be simultaneously reproduced unless **both** of the following conditions hold:

- The value of  $\gamma$  is greater than unity, implying that quasar luminosity is not a linear function of host mass.
- The observed clustering amplitude is in excess of that expected from dark matter halos ( $F > 1$ ), possibly implying that the observed bias is boosted because mergers trigger quasar activity.

The latter constraint on  $F$  is particularly strong. We find  $F > 1.1$  at the 99% level. On the other hand, we find that the scatter in the  $L - M$  relation can be constrained only to a value smaller than  $\sim 1$  dex (in difference from the recent study of White et al. 2008). We find that because of the weak constraint on the scatter the mean host mass can be only weakly constrained, to within an order of magnitude around  $\sim 10^{13} M_\odot$ . Importantly, and for the same reason, we find that clustering data combined with quasar densities does not constrain the quasar lifetime, as had been suggested previously (Martini & Weinberg 2001; Haiman & Hui 2001).

Interestingly, the literature already contains a physically motivated model which is consistent with all of the above constraints. A scenario in which galaxy mergers drive accretion onto a central black hole, which then radiates near its Eddington luminosity until it grows sufficiently to deposit (with a  $\sim 5\%$  efficiency) the binding energy of the surrounding gas over a dynamical time, yields an  $L-M$  relation with a value of  $\gamma = 5/3$  (Wyithe & Loeb 2003). For this value of  $\gamma$ , our constraints favor a value of  $1.5 \lesssim F \lesssim 2$ , which is consistent with estimates of the expected enhancement in clustering bias for merger driven activity of  $F \sim 1.5$  (Furlanetto & Kamionkowski 2006).

In summary, the clustering statistics combined with the luminosity function of high redshift quasars, provide compelling evidence for a scenario of merger-driven quasar activity, with black-hole growth that is limited by feedback. The resulting luminosity–halo mass relation implies that the luminosity to halo mass ratio increases with halo mass as expected in theoretical models that include feedback limited black hole growth.

**Acknowledgments.** The research was supported by the Australian Research Council (JSBW), by NASA grants NNX08AL43G and by Harvard University funds (AL).

## REFERENCES

- Adelberger, K. L., Steidel, C. C., Pettini, M., Shapley, A. E., Reddy, N. A., & Erb, D. K. 2005, ApJ, 619, 697

- Boyle, B. J., Shanks, T., Croom, S. M., Smith, R. J., Miller, L., Loaring, N., & Heymans, C. 2000, MNRAS, 317, 1014
- Bullock, J. S., Kolatt, T. S., Sigad, Y., Somerville, R. S., Kravtsov, A. V., Klypin, A. A., Primack, J. R., & Dekel, A. 2001, MNRAS, 321, 559
- Cooray, A. 2005, MNRAS, 364, 303
- Croom, S. M., Smith, R. J., Boyle, B. J., Shanks, T., Loaring, N. S., Miller, L., & Lewis, I. J. 2001a, MNRAS, 322, L29
- Croom, S. M., Shanks, T., Boyle, B. J., Smith, R. J., Miller, L., Loaring, N. S., & Hoyle, F. 2001b, MNRAS, 325, 483
- Croom, S. M., Boyle, B. J., Loaring, N. S., Miller, L., Outram, P. J., Shanks, T., & Smith, R. J. 2002, MNRAS, 335, 459
- Croom, S. M., et al. 2005, MNRAS, 356, 415
- Croton, D. J., Gao, L., & White, S. D. M. 2007, MNRAS, 374, 1303
- da Ángela, J., et al. 2008, MNRAS, 383, 565
- Di Matteo, T., Springel, V., & Hernquist, L. 2005, *Nature*, 433, 604
- Erb, D. K., Shapley, A. E., Steidel, C. C., Pettini, M., Adelberger, K. L., Hunt, M. P., Moorwood, A. F. M., & Cuby, J.-G. 2003, ApJ, 591, 101
- Fan, X., et al. 2001a AJ, 121, 54
- Fan, X., et al. 2001b AJ, 122, 2833
- Fan, X., et al. 2003, astro-ph/0301135
- Fan, X., et al. 2006, AJ, 132, 117
- Furlanetto, S. R., & Kamionkowski, M. 2006, MNRAS, 366, 529
- Gao, L., Springel, V., & White, S. D. M. 2005, MNRAS, 363, L66
- Gottlöber, S., Kerscher, M., Kravtsov, A. V., Faltenbacher, A., Klypin, A., Müller, V. 2002, A&A, 387, 778
- Haehnelt, M. G., Natarajan, P., & Rees, M. J. 1998, MNRAS, 300, 817
- Haiman, Z., & Loeb, A. 1998, ApJ, 503, 505
- Haiman, Z. & Hui, L. 2001, ApJ, 547, 27
- Hopkins, P. F., Hernquist, L., Cox, T. J., Robertson, B., & Krause, E. 2007, ApJ, 669, 45
- Hopkins, P. F., & Hernquist, L. 2008, arXiv:0809.3789
- Hopkins, P. F., Cox, T. J., Kereš, D., & Hernquist, L. 2008, ApJS, 175, 390
- Kauffmann, G. & Haehnelt, M. 2000, MNRAS, 311, 576
- Kauffmann, G., & Haehnelt, M. G. 2002, MNRAS, 332, 529
- King, A. 2003, ApJ. Lett., 596, L27
- Kolatt, T. S., et al. 1999, ApJL, 523, L109
- Kollmeier, J. A., et al. 2006, ApJ, 648, 128
- Komatsu, E., et al. 2008, ArXiv e-prints, 803, arXiv:0803.0547
- Lacey, C., & Cole, S. 1993, MNRAS, 262, 627
- Li, Y., et al. 2007, ApJ, 665, 187
- Lidz, A., Hopkins, P. F., Cox, T. J., Hernquist, L., & Robertson, B. 2006, ApJ, 641, 41
- Martini, P. 2003, preprint astro-ph/0304009
- Martini, P. & Weinberg, D. H. 2001, ApJ, 547, 12
- Mo, H. J., & White, S. D. M. 1996, MNRAS, 282, 347
- Murray, N., Quataert, E., & Thompson, T. A. 2005, ApJ, 618, 569
- Padmanabhan, N., White, M., Norberg, P., & Porciani, C. 2008, arXiv:0802.2105
- Percival, W. J., Scott, D., Peacock, J. A., & Dunlop, J. S. 2003, MNRAS, 338, L31
- Pettini, M., Shapley, A. E., Steidel, C. C., Cuby, J.-G., Dickinson, M., Moorwood, A. F. M., Adelberger, K. L., & Giavalisco, M. 2001, ApJ, 554, 981
- Porciani, C., & Norberg, P. 2006, MNRAS, 371, 1824
- Press, W. H., & Schechter, P. 1974, ApJ, 187, 425
- Richards, G. T., et al. 2006, AJ, 131, 2766
- Scannapieco, E., & Thacker, R. J. 2003, ApJL, 590, L69
- Shen, Y., et al. 2007, AJ, 133, 2222
- Sheth, R. K. & Tormen, G. 1999, MNRAS, 308, 119
- Sheth, R. K., Mo, H. J., & Tormen, G. 2001, MNRAS, 323, 1
- Silk, J., & Rees, M. J. 1998, Astron. Astrophys., 331, L1
- Tremaine, S., et al. 2002, ApJ., 574, 740
- Volonteri, M., Haardt, F., & Madau, P. 2003, ApJ, 582, 559
- Wake, D. A., Croom, S. M., Sadler, E. M., & Johnston, H. M. 2008, arXiv:0810.1050
- Wetzell, A. R., Cohn, J. D., White, M., Holz, D. E., & Warren, M. S. 2007, ApJ, 656, 139
- White, M., Martini, P., & Cohn, J. D. 2008, MNRAS, 1080
- Wyithe, J. S. B., & Loeb, A. 2003, ApJ., 595, 614
- Wyithe, J. S. B., & Loeb, A. 2005, ApJ, 634, 910
- Wyithe, J. S. B., & Padmanabhan, T. 2006, MNRAS, 372, 1681
- York, D. G. et al. 2000, AJ, 120, 1579